DOI: 10.1002/anie.200902182

Microfabrication

Microfluidic Formation of Monodisperse, Cell-Sized, and Unilamellar Vesicles**

*Sadao Ota, Satoko Yoshizawa, and Shoji Takeuchi**

Lipid vesicles are widely used as functional delivery vehicles in pharmaceuticals and cosmetics or as biochemical reactors that respond to various environmental stimuli.[1] Furthermore, as phopholipids are an integral part of biological membranes, phospholipid vesicles are attractive materials to mimic the complex biomembrane of cells. To efficiently use vesicles for these applications, the vesicle production methods are required to simultaneously control 1) unilamellarity, 2) encapsulation efficiency, and 3) vesicle size, which should be uniform and comparable to cell size. Unilamellar vesicles are required to study and control membrane behavior and transport through incorporated membrane proteins.[2,3] Vesicles that efficiently encapsulate a variety of biochemical components independently of the properties of the solution are necessary to produce effective delivery vehicles and minimal cells; encapsulation of concentrated biochemical compounds is needed to load sufficient amounts of chemicals into the vehicles and to realize conditions comparable to those in living cells.[4] Cell-sized vesicles offer desirable spatial and temporal scales to mimic the kinetic behavior of living cells.[5] Monodisperse vesicles facilitate quantitative analysis in laboratories and the controlled release of chemical compounds when used in industry. Thus, the production of vesicles with all of these properties significantly enhances their applicability, yet such species have remained elusive even with a variety of available technologies (Supporting Information, Table S1).[5–11]

Herein we demonstrate a technique for continuous generation of monodisperse cell-sized unilamellar vesicles from a microfluidic T junction. We began to reconstitute a lipid film in the junction by sequentially infusing water, oil, and water into the device. The cross flow at the T junction continuously thins, shears, and squeezes the membrane, and this membrane eventually releases multiple vesicles encapsulating uniform water droplets. This method has following advantages: 1) it produces monodisperse, cell-sized, unilamellar vesicles; 2) the encapsulation is efficient and versatile enough that a variety of contents can be used, including highly concentrated biochemical compounds; 3) microfluidics reduces the volume of reagents and enables high-throughput vesicle production. We demonstrate efficient encapsulation of concentrated compounds inside monodisperse vesicles as well as molecular transport through the functional pore proteins incorporated in the unilamellar membrane, and we investigate membrane properties by subjecting the vesicles to osmotic shock. Moreover, we encapsulate a cell-free gene expression system to build a cell-like reactor as a first step toward developing artificial cells.

A poly(dimethylsiloxane) (PDMS) device was fabricated using standard soft-lithographic techniques. We designed a main channel with a number of small chambers built into its walls. Each small chamber is further connected to a much larger chamber through a narrow channel (Figure 1). First, we filled the device with an aqueous solution while pushing air out through the PDMS walls (Figure 1a,b). This first solution later constitutes the content of the vesicles. Then, infused immiscible oil with dissolved phospholipids sweeps away the first solution in the channel but confines the rest in the chambers (Figure 1c). Last, another aqueous solution sweeps the oil away from the channel but eventually leaves an oil-containing lipid film in each small chamber (Figure 1d). In this film, amphiphilic lipid molecules self-assemble into two monolayers at both water–oil interfaces. By inducing the fluid in the chamber to flow outward, the film bends and further thins down, resulting in contact of the two monolayers; these layers become a bilayer (Figure 1e).[12] To induce the outward flow, we pattern aluminum in the large chamber and heat it with an infrared laser to generate a microbubble.[13] The narrow channel connecting the small and large chamber is designed to have a high fluidic resistance, and this resistance prevents the bubble from swelling rapidly and subsequently slows the outward flow. Eventually, we were able to accomplish a sufficiently gentle deformation of the lipid bilayer without breaking it up. Finally, high shear forces from the continuous fluid stream pinch off the leading edge of the deformed bilayer to form monodisperse unilamellar vesicles (Figure 1f–h and Figure 2a).

Since the original bilayer remained intact during the course of the experiment, multiple vesicles were produced continuously. By maintaining a constant flow rate, the vesicles generated from one chamber showed a narrow size distribution whose coefficient of variation (CV) was less than 5%

[*] S. Ota, Prof. S. Takeuchi
Institute of Industrial Sciences, University of Tokyo
4-6-1 Komaba, Meguro-ku, Tokyo 153-8505 (Japan)
Fax: (+81) 3-5452-6649
E-mail: takeuchi@iis.u-tokyo.ac.jp
Prof. S. Takeuchi
PRESTO, JST
4-1-8 Honcho, Kawaguchi, Saitama 332-0012 (Japan)
Dr. S. Yoshizawa
LIMMS/CNRS-IIS (UMI2820), University of Tokyo
4-6-1 Komaba, Meguro-ku, Tokyo 153-8505 (Japan)

[**] We thank Dr. Andrew S. Utada for helpful discussions. This work was partly supported by Grants-in-Aid for Scientific Research on Priority Areas (innovative nanoscience) from Ministry of Education, Culture, Sports, Science, and Technology Japan and Kanagawa Academy of Science and Technology (KAST) (Japan).

Supporting information for this article is available on the WWW under http://dx.doi.org/10.1002/anie.200902182.

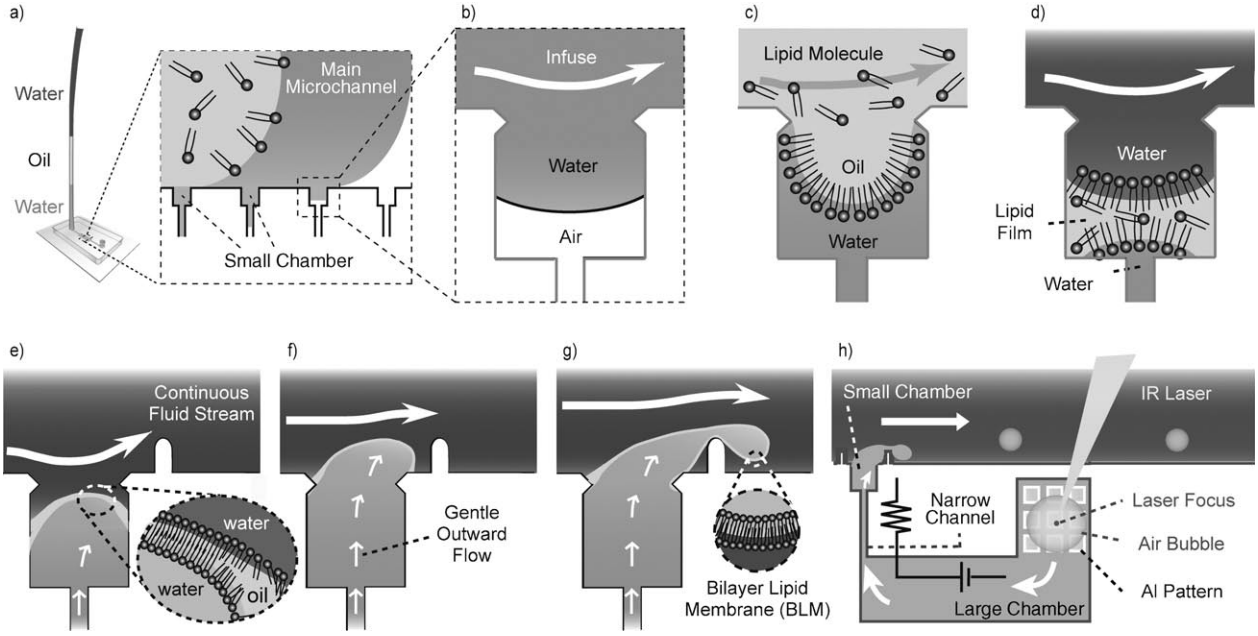

Figure 1. Microfluidic process for the generation of monodisperse unilamellar vesicles. a) Water, oil with dissolved lipids, and water are sequentially infused into a microfluidic device, in which a main channel has many chambers in its walls. b) Water fills the device while pushing air out through the PDMS wall. c) Oil flushes away the water in the channel, but confines the remaining water in the chambers. d) Water again flushes away the oil, and the residue forms an oil film in which amphiphilic lipid molecules form two monolayers at the interface of water and oil. e)–g) Schematic depiction of the flow-driven unilamellar vesicle formation. e) A cross flow at the microfluidic T junction thins the lipid film and drives the contact of monolayers to form a bilayer. f) The gentle outward flow further bends out the bilayer. g) Shear forces from the continuous fluid stream lead to the fission of the leading edge of the bilayer, that is, the generation of a unilamellar vesicle. h) The system integrated with an optically generated microbubble.

(Figure 2b,c and Supporting Information, Video S1). We confirmed the robustness of the vesicles by observing the vesicles over several days after formation.

A time-series measurement of the vesicle diameters by video microscopy offers insight into the mechanism of fission at the T junction. We investigated the relationship between the rate of outward flow Q from a single chamber and the diameter of the vesicles. In this case, Q was calculated by dividing the volume of each vesicle by the time interval between vesicle formation events. As a result, we found that vesicle size was independent of Q (Figure 2d). In contrast, once the formation of vesicles began, their size varied with changes in the external flow rate (data not shown). We also found that the size of the vesicles gradually increased with time, although this change proceeded slowly enough to maintain the size monodispersity (Figure 2e). Abundant lipid molecules within the solvent remaining on the channel surfaces replenished the original bilayer, enabling the formation of vesicles in rapid and continuous succession. However, since the concentration of the lipids in the oil film decreased as vesicles were generated, the surface tension increased, resulting in an increase in vesicle size. These results led us to postulate that vesicle size is defined as a result of the competition between the shear forces exerted by external flow and the surface tension mainly determined by the concentration of the lipid molecules.[10,14] In our case, the flow of the discontinuous phase was much slower than that of the continuous phase around the vesicle, and therefore Q might not affect the competition. We can observe similar behaviors when generating water droplets in oil within the T junction device and can explain the mechanism in the same way.[10] An important advantage of our approach is that the internal and external fluids are completely separated when a vesicle is formed, thus enabling highly efficient encapsulation. As this technique depends only on a large physical deformation of the lipid bilayer, we expect that the efficiency of encapsulation is independent of the specific properties of the encapsulated solutes, such as molecular weight, charge, and concentration. As a demonstration, we loaded a high concentration of fluorescent beads (200 nm in diameter) dissolved in phosphate-buffered saline (PBS) into the vesicles. A confocal microscope allowed us to take images of encapsulated beads appearing in the same plane (Figure 2f). We determined the average number of beads that appeared within the same 8 μm square area in 20 images taken at 300 ms intervals. The average number of beads in each vesicle was constant in over 22 vesicles (Supporting Information, Video S2 and Figure S1). Furthermore, we compared the number of encapsulated beads with that in the original bulk solution. As a result, the concentration of the beads within the vesicles was almost the same as the original one. These results indicate that our technique enables a highly reproducible and efficient encapsulation of solutes and macromolecules within the monodisperse vesicles.

To investigate the membrane properties of the vesicles, we added α-hemolysin monomers to a solution surrounding the vesicle that encapsulated calcein fluorescent molecules at 10 mM (Figure 3a). α-Hemolysin is a toxic membrane protein

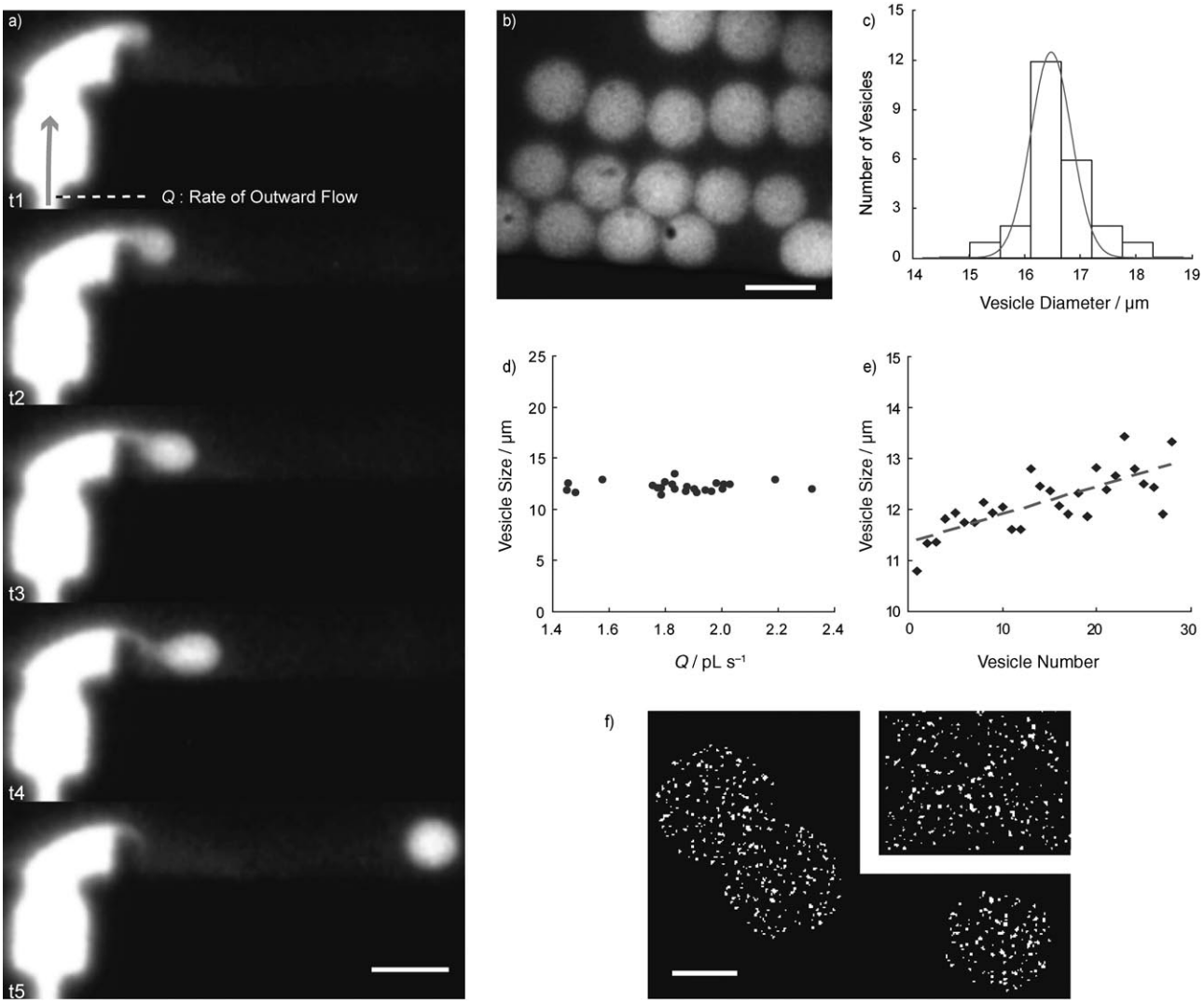

Figure 2. Flow-driven formation of monodisperse vesicles and insight into the mechanisms of their breakup. a) Flow-driven vesicle formation. Individual fluorescence images t1–t5 were sequentially taken from a high-speed movie (250 fps). The vesicles encapsulated 10 mM fluorescent calcein. Scale bar: 20 μm. b) Fluorescence image of the generated vesicles. Scale bar: 20 μm. c) Homogeneous distribution of the vesicle size measured in (b) ($n = 24$, mean = 16.5 μm, CV = 3.70%). The mean size of the monodisperse vesicles varied between different chambers. d), e) The time-series measurement of the vesicle diameters indicates the mechanism governing the flow-driven formation ($n = 28$, mean = 12.1 μm, CV = 4.83%). d) Small correlation between vesicle diameter and the rate of outward flow illustrated in (a) (correlation coefficient = −0.0879). e) Gradual increase in vesicle size with time. f) Efficient encapsulation was confirmed by comparing the concentration of the fluorescent beads of the encapsulated contents (left) and that of the original bulk solution (upper right) using confocal microscopy. Scale bar: 10 μm.

whose monomers are known to bind to unilamellar biomembranes and oligomerize to form water-filled transmembrane nanopores.[15] With the incorporation of this protein, calcein molecules started to diffuse out through the nanopores that formed across the membrane. Owing to the small volume of the vesicles, such membrane transport was readily observed as changes in the fluorescence intensity of the vesicle (Figure 3a, b). This result confirms that the membrane of the vesicle is unilamellar, indicating the feasibility of engineering the properties of such a membrane.

Although we demonstrated the functional properties of the unilamellar vesicles, we suspect that the membranes are heterogeneous, as the vesicles are produced from an artificial lipid membrane containing oil. To investigate how trapped oil affects the membrane properties, we subjected vesicles of various sizes to an osmotic pressure shock by introducing glucose at a high final concentration of approximately 200 mM. The vesicles generated from different chambers and encapsulating 10 mM calcein had diameters of 18, 25, and 31 μm. The osmotic pressure of glucose pumped water out of the vesicles through the membrane, causing them to shrink gradually. However, this shrinkage increased the concentration of loaded solutes starting at 158 mM, subsequently reducing osmotic pressure. As a result, the decrease in vesicle size slowed and eventually stopped when the pressure was balanced across the membrane (Figure 3c). We found that vesicles of various sizes shared similarities in the initial rate of change in the vesicle radius R (Figure 3d). The reduction of

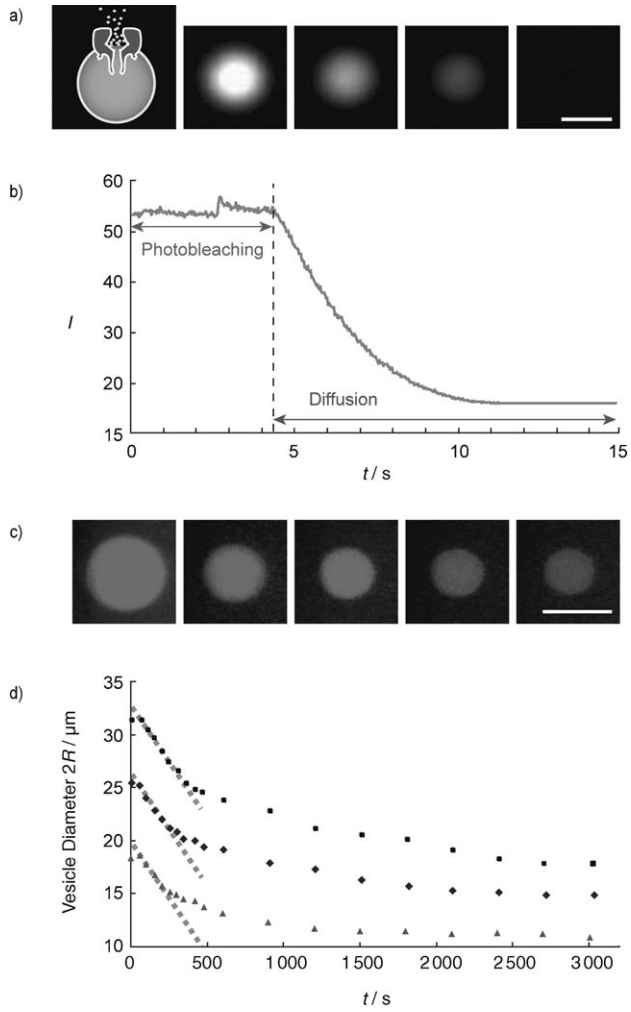

Figure 3. Characterization of vesicle membranes. a), b) Molecular transportat across the unilamellar membrane through α-hemolysin nanopores. a) Schematic diagram (left) and sequential images (right) of the decrease in the fluorescence intensity of a vesicle arising from the diffusion of calcein molecules through transmembrane nanopores. Individual frames were taken from a fluorescence-enhanced movie immediately after the start of diffusion at equal intervals of 2.5 s. (Scale bar: 10 μm.) b) Kinetics of fluorescence intensity of a vesicle. c), d) Evolution of vesicles under osmotic pressure shock induced by adding concentrated glucose to the surrounding liquids. Before the addition, the vesicle radius was constant. After the addition, the resultant osmotic pressure across the membrane pumped water out of the vesicles, causing them shrink. c) Sequential images showing the evolution of a 31 μm diameter vesicle at equal intervals of 600 s. Scale bar: 30 μm. d) Radius of three different vesicles of different diameters (18 (▲), 25 (◆), and 31 μm (■)). The vesicles were formed from three different chambers, collected together, and subjected to the same osmotic pressure. The vesicles showed a similar permeability that was deduced from the initial slope (dotted gray lines) using Equation (1).

the pressure with the gradual increase in solute concentration was small enough to be neglected for a short time. Therefore, we determine the permeability of the membrane P as in Equation (1):

$$\frac{dR}{dt} \approx -\alpha P \Delta c \qquad (1)$$

where α is the molar volume of water ($\alpha = 18 \times 10^{-3}\,\mathrm{L\,mol^{-1}}$) and Δc ($\mathrm{mol\,L^{-1}}$) is the difference in glucose concentration between the inner and outer solutions.[16] From the initial slope drawn between 60 and 205 s for the three different vesicles, we determined that $P \approx 13.0$, 15.7, and 14.9 $\mu\mathrm{m\,s^{-1}}$. These values were slightly smaller than that measured for conventionally formed phospholipid vesicles ($P \approx 15$–$150\ \mu\mathrm{m\,s^{-1}}$).[17] Although we noticed that the trapped solvent in the membrane altered the permeability, previous studies successfully demonstrated the use of these vesicles to mimic cellular functions.[5] Furthermore, the differently sized vesicles showed similar permeabilities to water, indicating their applicability to the quantitative study of membrane transport.

Finally, we demonstrated the functionality of the vesicles as cell-sized bioreactors.[5,6] We encapsulated a cell-free gene expression system from *Escherichia coli* in phospholipid vesicles. The continuous aqueous phase was a feeding solution containing a buffer with nutrients (mainly ribonucleotides and amino acids). Expression of the green fluorescent protein (GFP) gene was monitored by measuring fluorescence intensity inside a vesicle. Each vesicle was kept in the device at room temperature (25 °C). As a result, we observed a continuous expression of fluorescent GFP molecules that lasted for more than five hours (Figure 4). The sequential images shown in Figure 4 b were taken 0, 1, 2, 5, and 15 h after the encapsulation. This result also demonstrated that we can encapsulate a solution as complex as a cell-free extract in a vesicle. To date, this encapsulation has been difficult since highly concentrated proteins interfere with phospholipids when they form interfacial membranes.[18]

We anticipated that the heating to form microbubbles could denature biomolecules. To avoid this denaturation, we designed the device such that the point of heating is separated

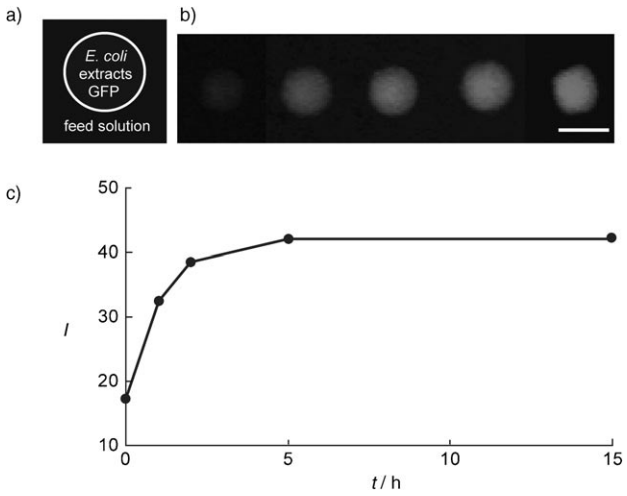

Figure 4. Encapsulation of *E. coli* extracts and expression of GFP. a) Schematic depiction of encapsulation of *E. coli* extracts for expression of GFP. The *E. coli* extract, a plasmid containing GFP gene, and nutrients for the protein synthesis were encapsulated in the vesicles surrounded by the same nutrient-containing buffer (feed solution). b) Sequential images of the vesicle fluorescence of GFP, corresponding to 0, 1, 2, 5, and 15 h after starting observation by optical microscopy. Scale bar: 20 μm. c) Kinetics of the expression of GFP inside the vesicle.

from the junction. Moreover, the external flow continuously removes the generated heat. Indeed, we successfully demonstrated the feasibility of performing in-vitro transcription and translation inside the vesicles. The simplest way to further avoid the heating problem is to use other methods to deform the bilayer while maintaining the main concept of this technique; for example, a microbubble generated by electrolysis or a pressure-driven pump can be used to precisely supply controlled force onto the bilayer.

The number of vesicles produced from one bilayer was limited to around 50–100 and might be slightly smaller than what is expected for microfluidics. However, since we form an array of lipid films in the microfluidic channel, thousands of vesicles can be produced within a device. Furthermore, we believe that supplying the original bilayer with an adequate volume of lipid solution makes it possible to prepare thousands of monodisperse vesicles from a bilayer. Once the infinitely continuous formation method is realized, we expect that it will be able to control vesicle size simply by changing the flow rate.

In conclusion, we have presented a microfluidic technique for generating cell-sized unilamellar monodisperse vesicles that efficiently encapsulate concentrated solutes and macromolecules. The technique uses a small volume of encapsulated reagents (1–3 μL) and enables high-throughput production of hundreds of vesicles per minute. The vesicles can be observed immediately after formation and have a long lifetime of more than several days. These obtained features markedly expand the applicability of vesicles in various fields.[1–5,19] Simultaneous control of the composition of the lipid membrane, encapsulated content, and the surrounding liquid will give access to engineered vesicles that controllably interact with and respond to environmental stimuli. In particular, such vesicles with uniform diameters ranging from 1 to 30 μm will be good models to mimic complex functions of cells with appropriate temporal and spatial scales. Furthermore, these vesicles can be directly manipulated with functional microfluidic designs and therefore provide a straightforward route for the quantitative study of multicomponent biomolecular systems in a lab-on-a-chip device. Moreover, we believe that the generality of our method is applicable to the fabrication of various hollow structures, including shells, vesicles, and polymerosomes.

Received: April 23, 2009
Published online: July 30, 2009

Keywords: artificial cells · lipid bilayers · microfluidics · synthetic biology · vesicles

[1] a) D. D. Lasic, D. Papahadjopoulos, *Science* **1995**, *267*, 1275–1276; b) P. Walde, *Curr Opin. Colloid Interface Sci.* **1996**, *1*, 638–644.
[2] T. Baumgart, S. T. Hess, W. W. Webb, *Nature* **2003**, *425*, 821–824.
[3] Y. Tamba, M. Yamazaki, *Biochemistry* **2005**, *44*, 15823–15833.
[4] a) I. A. Chen, R. W. Roberts, J. W. Szostak, *Science* **2004**, *305*, 1474–1476; b) J. D. Mitchel, L. S. Michael, *Mol. Syst. Biol.* **2007**, *3*, 125.
[5] V. Noireaux, A. Libchaber, *Proc. Natl. Acad. Sci. USA* **2004**, *101*, 17669–17674.
[6] a) J. P. Reeves, R. M. Dowben, *J. Cell. Physiol.* **1969**, *73*, 49–60; b) F. Olson, C. A. Hunt, F. C. Szoka, W. J. Vail, D. Papahadjopoulos, *Biochim. Biophys. Acta* **1979**, *557*, 9–23; c) M. I. Angelova, D. S. Dimitrov, *Faraday Discuss.* **1986**, *81*, 303–311; d) M. Karlsson, et al., *Anal. Chem.* **2000**, *72*, 5857–5862; e) F. Szoka, D. Papahadjopoulos, *Proc. Natl. Acad. Sci. USA* **1978**, *75*, 4194–4198.
[7] S. Pautot, B. J. Frisken, D. A. Weitz, *Proc. Natl. Acad. Sci. USA* **2003**, *100*, 10718–10721.
[8] a) K. Funakoshi, H. Suzuki, S. Takeuchi, *J. Am. Chem. Soc.* **2007**, *129*, 12608–12609; b) J. C. Stachowiak, D. L. Richmond, T. H. Li, A. P. Liu, S. H. Parekh, D. A. Fletcher, *Proc. Natl. Acad. Sci. USA* **2008**, *105*, 4697–4702.
[9] H. C. Shum, D. Lee, I. Yoon, T. Kodger, D. A. Weitz, *Langmuir* **2008**, *24*, 7651–7653.
[10] T. Thorsen, R. Roberts, F. Arnold, S. Quake, *Phys. Rev. Lett.* **2001**, *86*, 4163–4166.
[11] A. S. Utada, E. Lonrenceau, D. R. Link, P. D. Kaplan, H. A. Stone, D. A. Weitz, *Science* **2005**, *308*, 537–541.
[12] a) K. Funakoshi, H. Suzuki, S. Takeuchi, *Anal. Chem.* **2006**, *78*, 8169–8174; b) H. Suzuki, K. V. Tabata, H. Noji, S. Takeuchi, *Langmuir* **2006**, *22*, 1937–1942.
[13] W. H. Tan, S. Takeuchi, *Proc. Natl. Acad. Sci. USA* **2007**, *104*, 1146–1151.
[14] C. D. Eggleton, T. M. Tsai, K. J. Stebe, *Phys. Rev. Lett.* **2001**, *87*, 048302.
[15] L. Song, M. Hobaugh, C. Shustak, S. Cheley, H. Bayley, *Science* **1996**, *274*, 1859–1865.
[16] E. Lorenceau, A. S. Utada, D. R. Link, G. Cristobal, M. Joanicot, D. A. Weitz, *Langmuir* **2005**, *21*, 9183–9186.
[17] a) B. M. Discher, Y. Y. Won, D. S. Ege, J. C. Lee, F. S. Bates, D. E. Discher, D. A. Hammer, *Science* **1999**, *284*, 1143–1146; b) H. O. Negrete, R. L. Rivers, A. H. Goughs, M. Colombini, M. L. Zeidel, *J. Biol. Chem.* **1996**, *271*, 11627–11630.
[18] F. Divet, G. Danker, C. Misbah, *Phys. Rev. E* **2005**, *72*, 041901.
[19] G. Sessa, G. Weissman, *J. Biol. Chem.* **1970**, *245*, 3295–3301.

